International Journal of Nanomedicine

Dovepress
open access to scientific and medical research

Open Access Full Text Article

ORIGINAL RESEARCH

# Electrochemical Deposition of Nanostructured Hydroxyapatite Coating on Titanium with Enhanced Early Stage Osteogenic Activity and Osseointegration

This article was published in the following Dove Press journal:
*International Journal of Nanomedicine*

Minxun Lu[1,2]
Hongjie Chen[2]
Bo Yuan[2]
Yong Zhou[1]
Li Min[1]
Zhanwen Xiao[2]
Xiangdong Zhu[2]
Chongqi Tu[1]
Xingdong Zhang[2]

[1]Department of Orthopedics, West China Hospital, Sichuan University, Chengdu, People's Republic of China; [2]National Engineering Research Center for Biomaterials, Sichuan University, Chengdu, People's Republic of China

**Purpose:** The aim of research is to fabricate nanostructured hydroxyapatite (HA) coatings on the titanium via electrochemical deposition (ED). Additionally, the biological properties of the ED-produced HA (EDHA) coatings with a plate-like nanostructure were evaluated in vitro and in vivo by undertaking comparisons with those prepared by acid/alkali (AA) treatment and by plasma spray-produced HA (PSHA) nanotopography-free coatings.

**Materials and Methods:** Nanoplate-like HA coatings were prepared through ED, and nanotopography-free PSHA coatings were fabricated. The surface morphology, phase composition, roughness, and wettability of these samples were investigated. Furthermore, the growth, proliferation, and osteogenic differentiation of MC3T3-E1 cells cultured on each sample were evaluated via in vitro experiments. Histological assessment and push-out tests for the bone–implant interface were performed to explore the effect of the EDHA coatings on the interfacial osseointegration in vivo.

**Results:** XRD analysis showed that the strongest intensity for the EDHA coatings was at the (002) plane rather than at the regular (211) plane. Relatively higher surface roughness and greater wettability were observed for the EDHA coatings. Cellular experiments revealed that the plate-like nanostructured EDHA coatings not only possessed an ability, similar to that of PSHA coatings, to promote the adhesion and proliferation of MC3T3-E1 cells but also demonstrated significantly enhanced early or intermediate markers of osteogenic differentiation. Significant osseointegration enhancement in the early stage of implantation period and great bonding strength were observed at the interface of bone and EDHA samples. In comparison, relatively weak osseointegration and bonding strength of the bone–implant interface were observed for the AA treatment.

**Conclusion:** The biological performance of the plate-like nanostructured EDHA coating, which was comparable with that of the PSHA, improves early-stage osteogenic differentiation and osseointegration abilities and has great potential for enhancing the initial stability and long-term survival of uncemented or 3D porous titanium implants.

**Keywords:** electrochemical deposition, hydroxyapatite coatings, nanoscale, osteogenic activity, osseointegration

Correspondence: Xiangdong Zhu
National Engineering Research Center for Biomaterials, Sichuan University, No. 29 Wangjiang Road, Chengdu 610064, People's Republic of China
Tel +86-28-85470770
Email zhu_xd1973@scu.edu.cn

Chongqi Tu
Department of Orthopedics, West China Hospital, Sichuan University, No. 37 Guoxue Street, Chengdu 610041, People's Republic of China
Tel +86-28-85422570
Email Tuchongqi@yeah.net

## Introduction

Titanium (Ti) and its alloys are considered to be an ideal metallic biomaterials and are widely used for bone repair because of their excellent fatigue and corrosion

resistance along with high strength-to-weight ratio.[1,2] Despite the impressive developments that have been achieved in the field of metallic biomaterials for orthopedic use, the inherent bio-inert nature of Ti is still a problem with regard to the promotion of bone healing and integration between the host bone and the implant. Delayed bone healing and weak osseointegration at the bone–implant interface affect both the primary and secondary stability of implants, and also increase the risk of aseptic loosening. Besides the poor bioactivity of Ti, a mismatch of Young's modulus, also known as stress shielding, between the dense Ti and bone has been recognized as another critical reason for implant loosening. However, the use of porous Ti may provide an alternative solution for stress shielding because the porous structure can effectively decrease the stiffness discrepancy.[3] Furthermore, several studies have demonstrated enhanced osteogenic activity in using porous Ti.[4] Despite the use of porous Ti, interfacial osseointegration is still hard to maximize due to the bio-inertness of Ti. Various approaches have been studied to modify the biological inertness of the Ti surface, and to augment further osteogenesis and bone ingrowth. Currently, three major types of surface modification have been examined, including chemical or electrochemical treatment, biomimetic mineralization, and fabrication of bioactive coatings.[5–8]

The application of chemical treatment permits the conversion of dense or porous Ti into a bioactive material in a relatively simple and cost-effective way. In an early study, alkali-heat treatment was used to form a bioactive layer of sodium titanate on the Ti surface.[9] Even though the bioactivity of alkali- and heat-treated Ti could be further enhanced by the removal of sodium,[10] subsequent heat treatment still had a negative effect on the bioactivity of the substrate materials. Initiation of apatite nucleation would be significantly affected by the loss of Ti-OH groups under high temperatures.[11] Numerous studies have focused on the development of acid-alkali (AA) treatments where thermal effects are absent. Zhao et al confirmed a faster osteoinduction in the AA treatment compared to chemical-thermal treatment.[12] Compared to NaOH-treated samples, the NaOH, HCl, and water-treated samples exhibited better bioactivity.[10] Moreover, subsequent studies suggested that the anatase and titanate hydrogen layers without Na were also formed on a sodium-free surface of Ti by the AA treatment, and could facilitate the enhancement of bioactivity.[13,14] Although the AA treatment might be considered to be an acceptable method for fabricating bioactive Ti implants, a bio-ceramic coating that can release calcium and phosphorus ions to activate bone regeneration would seem to be a better choice to further enhance the bioactivity of Ti.

For ceramic coatings, hydroxyapatite (HA) has been demonstrated to be a reliable and an effective material because of its similarity with the mineral phase of natural bone tissue.[15] Numerous methods are available for preparation of HA coatings, such as plasma spraying (PS), biomimetic deposition, sol–gel deposition, and electrochemical deposition (ED).[6,16-19] Although PS is the preferred method in most cases due to its convenience, high repeatability, and efficiency, its excessively high temperatures (≥15,000°C) and the subsequent rapid cooling procedure generate a large amount of amorphous HA,[20] and consequently there are variations in the structure of HA.[21,22] In addition, the interior coating of the 3D porous structure is not accessible due to the line-of-sight nature of the spraying process. Given the increasing clinical demand for porous implants, there is much interest in developing non-line-of-sight deposition processes. Biomimetic deposition allows for the production of homogeneous HA coatings on complex porous scaffolds, and functional and biological agents, such as growth factors, could be incorporated in HA coatings because of the near physiological conditions employed in biomimetic deposition. However, the thickness, the formation rate, and the quality of the coating are difficult to control using biomimetic method, and the bonding strength of the coating is also unacceptable.[17,23] Low temperature ($T < 100°C$) ED is a versatile technique capable of delivering an HA coating on porous Ti with satisfactory homogeneity, thickness, and bonding strength. Furthermore, this technique can not only overcome the phase transition problems of PS-fabricated HA coatings but also the morphology of the HA coating can be modified by adjustment of the ED parameters.

Topographic modification is another important approach for improving the biological response and osseointegration ability of HA coatings. According to recent research, it is accepted that nanostructured surfaces accelerate and augment osteoblast adhesion, cell proliferation, and cell differentiation,[24–26] as well as stimulate angiogenic factor secretion.[27,28] Recently, specific modified-surface nanostructures, such as nanotubes, nanorods, nanowires, and nanofibers, have been reported.[29] But, most of these structures are the results of Ti surface modification rather than a morphology change of the HA coating and are mainly aimed at addressing the relatively low adhesive strength of the coating on the substrates and delaminates of ceramic coatings. However, AA pre-treatment also could be an option for solving the problems of weak adhesion and delamination of HA coatings. Such AA-treated surfaces have been characterized as

a bioactive $TiO_2$ layer with the mixture of a micro/nanoscale network-like topography, which provides the ideal fundamental substrate for HA deposition. Based on these structures, nanoplate-like and nanorod-like HA coatings were successfully prepared via the ED method combined with AA pretreatment, and their positive effects on biocompatibility were initially confirmed in our previous study.[30] To date, no study has systemically examined the superior biological properties of nanoplate-like HA coatings on an AA-treated substrate, especially in terms of the osteogenic activity and osseointegration, which are critical factors affecting the lifespan of implants.

The aim of this study is to understand the effects of nanostructured EDHA coatings on AA-treated Ti implants towards the early stage osteogenic activity and osseointegration in vitro and in vivo by undertaking comparisons with nanotopography-free PS-produced HA coatings and ceramic coating-free AA treatments. The growth, proliferative rate, and osteo-specific gene expression of MC3T3-E1 cells cultured on each sample category have been investigated. Adult beagles were implanted with each sample category for 6 and 12 weeks. The implant bone specimens were characterized by histological imaging, histomorphometric analysis, and by mechanical push-out tests to measure the influence of the nanoplate-like HA coating on early-stage osseointegration.

## Materials and Methods

### Preparation of Various Surface-Modified Ti Samples

Dense Ti disks (14 mm diameter × 1 mm height, Figure 1A) were used in this study. In brief, the surfaces of the Ti disks were polished with SiC paper, and then rinsed sequentially with ethanol, acetone, and deionized water. Next, the discs were etched with 4 M $HNO_3$ at 40°C for 1 h. The etched samples were then washed with deionized water until a neutral pH was attained, and subsequently, immersed in a 5 M NaOH solution at 60°C for 10 h. After washing gently in deionized water, the samples were dried at 40°C for 24 h. The AA-treated Ti samples were named as AA-Ti.

To obtain the nanostructured HA coating, ED was performed on the AA pre-treated Ti samples using an electrochemical workstation (PARSTAT 2273, Princeton Applied Research, USA), wherein a metallic substrate was used as the cathode, a graphite rod served as the anode, and a saturated calomel electrode (SCE) was employed as the reference electrode. The anode and cathode were connected to a DC power source. A 5 cm long compartment between the electrolyte inlet/outlet and the anode/cathode was made to ensure laminar electrolyte flow in the ED system. The electrolyte consisted of $Ca(NO_3)_2$ and $(NH_4)H_2PO_4$, with concentrations of calcium and phosphorus of 2.5 mM and 1.5 mM, respectively. The pulse current density was 5 mA/cm$^2$. In accordance with the previous study,[30] 90 cycles of deposition ($t_d$ = 1 s) were applied followed by a 10 s break. The deposition conditions were as follows: pH = 6.5, T = 70°C, stirring speed = 200 rpm, and deposition time = 2 h. The ED products were named EDHA-Ti.

For the preparation of the PS-produced HA coating, spherical HA powders with average particle size below 70 μm and calcined at 1250°C for 2 h were spray-coated on a sandblasted Ti substrate in an atmospheric PS system

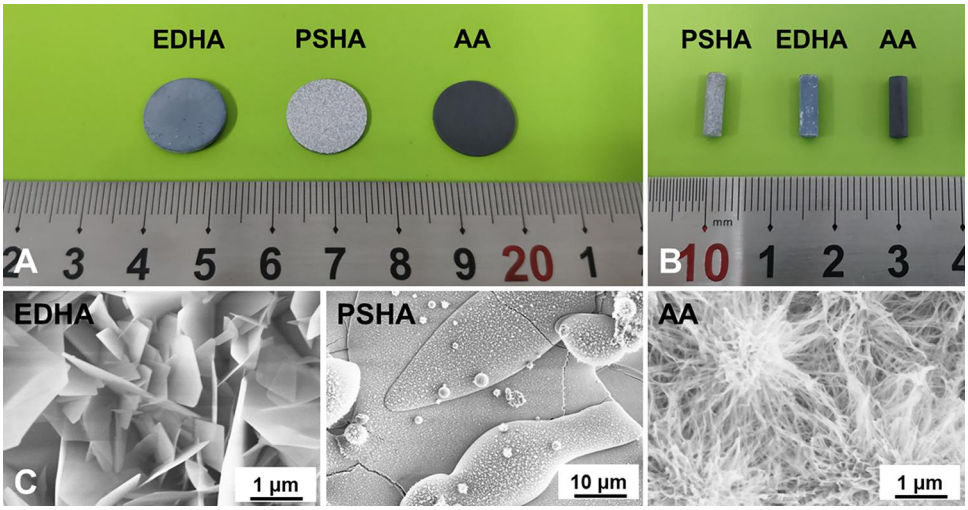


**Figure 1** Digital photographs of surface-modified titanium disks (**A**) and implants (**B**) used in vitro and vivo experiments, respectively; (**C**) SEM images of the titanium samples with different surface modifications.

(Shanghai Dahao Corporation, China). The resulting HA coatings were then subjected to hydrothermal treatment in a pulse vacuum sterilizer (SHINVA, China), and the final samples were termed PSHA-Ti.

## Surface Characterization

The morphologies of the surface coatings of the samples were investigated by field emission scanning electron microscopy (FE-SEM, S4800, Hitachi, Japan). Furthermore, the phase compositions of the coatings were determined by thin-film X-ray diffraction (TF-XRD, X'pert pro-MPD, PANalytical, Netherlands). The surface topography and wettability of the coatings were evaluated using an atomic force microscope (AFM, MFP-3D, Asylum Research, USA) and a contact angle meter (DSA-100, Kruss, Germany), respectively.

## In vitro Study

### Cell Culture

Mouse pre-osteoblast cell lines (MC3T3-E1) were purchased from the Cell Bank of the Chinese Academy of Sciences (Shanghai, China), and selected to explore the osteogenic activity of EDHA-Ti, PSHA-Ti, and AA-Ti. The cells were cultured in an α-minimum essential medium (α-MEM, Hyclone, USA) supplemented with 10% fetal bovine serum (FBS, Gibco), 100 U/mL penicillin, and 100 mg/mL streptomycin (Sigma, USA) in an incubator at 37°C with 5% $CO_2$. The culture medium was renewed every two days. After sample sterilization with 75% ethanol for 1.5 h, a total of $2.0 \times 10^4$ cells were seeded onto each sample in a 24-well plate for each test. For each experiment, at least three replicate samples were used.

### Cell Growth

The growth of MC3T3-E1 cells on each sample was observed by an inverted confocal laser scanning microscope (CLSM, TCS SP 5, Leica Microsystems, Germany). After 1, 3, and 5 days of culture, the samples were washed with phosphate-buffered saline (PBS) and stained with 0.1% fluorescein diacetate (FDA, Topbio Science, China) and propidium iodide (PI, Sigma, USA) for 2 min. Living cells were visualized as fluorescent green spots, whereas apoptotic cells were observed as fluorescent red spots in the CLSM images.

### Cell Proliferation

Cell proliferation was investigated by using the cell counting kit-8 assay (CCK-8, DOJINDO, Japan). After 1, 3, and 5 days of cell culture, the samples were collected, and gently washed to remove the apoptotic cells attached on the sample surfaces. Then, the samples were placed into a new 24-well plate filled with 500μL α-MEM medium containing 10% CCK-8 factor per well, and cell culture was continued for 2 h at 37°C in the dark. The supernatants were then collected and transferred to a 96-well plate to measure the absorbance of each pore at a wavelength of 450 nm in a microplate reader (VarioskanFlash, ThermoScientific, USA).

### Osteogenic Gene Expression

The effects of AA-Ti, EDHA-Ti, and PSHA-Ti on the osteogenic gene expression of alkaline phosphatase (ALP), bone sialoprotein (BSP), collagen I (Col-I), osteocalcin (OCN), and osteopontin (OPN) were investigated using real-time quantitative polymerase chain reaction (RT-qPCR). Glyceraldehyde 3-phosphate dehydrogenase (GAPDH) was used as a reference marker. Table 1 lists the primers for the osteogenic markers. After 7 and 14 days of culture, the ribonucleic acid (RNA) of the attached cells was extracted from the cells using the TRIzol reagent (Invitrogen, USA), according to the specifications. Subsequently, the RNA was reversely transcribed into cDNA using the iScript cDNA synthesis kit (Bio-Rad, USA). The equivalent cDNA was collected and transcribed into mRNA in PCR tube strips using a CFX96 real-time thermocycler (Bio-Rad, USA). The mRNA expression level of osteoblast-associated protein was analyzed using the ΔΔCt method.

**Table 1** The Primer Sequences for the Osteogenic Genes

| Gene | Forward Primer Sequence | Reverse Primer Sequence |
|---|---|---|
| *GAPDH* | ACCCAGAAGACTGTGGATGG | CACATTGGGGGTAGGAACAC |
| *ALP* | CCAGCAGGTTTCTCTCTTGG | GGGATGGAGGAGAGAAGGTC |
| *BSP* | CAGGGAGGCAGTGACTCTTC | AGTGTGGAAAGTGTGGCGTT |
| *Col-I* | GAGCGGAGAGTACTGGATCG | GTTCGGGCTGATGTACCAGT |
| *OCN* | GGACCATCTTTCTGCTCACTCTG | TTCACTACCTTATTGCCCTCCTG |
| *OPN* | TCTGATGAGACCGTCACTGC | AGGTCCTCATCTGTGGCATC |

## In vivo Study

### Material Preparation

Cylindrical EDHA-Ti, PSHA-Ti, and AA-Ti implants (3 mm diameter × 10 mm height, Figure 1B) were used for the in vivo study. For each category of implants, there were at least 16 implants.

### Surgery and Implantation Procedure

The animal study was approved by the Institutional Animal Care and Use Committee (West China Hospital, Sichuan University, Chengdu, China) and all procedures of this study were performed according to the Guide for the Care and Use of Laboratory Animals of Sichuan University. A total of 12 adult beagle dogs (6 females and 6 males, weight 11–13 kg) were obtained from the Laboratory Animal Center of Sichuan University (Chengdu, China). The animals were anaesthetized by intramuscular injection of propofol (4 mg/kg). Under sterile conditions, the distal femur was well exposed using a lateral approach. Using a dental drill, a hole (3 mm diameter, 10 mm depth) was prepared transversely at the femoral shaft and the condylar, respectively. To prevent thermal necrosis of bone, low-speed drilling and continuous saline irrigation were performed. Finally, the samples were gently implanted into the drilled holes. The 12 beagles as-operated on were randomly divided into three groups to receive the AA-Ti, the EDHA-Ti, and the PSHA-Ti implants, respectively. After 6 weeks of implantation, two beagles in each group were euthanized by using an over-dosage of sodium pentobarbital and saturated potassium chloride solution. The remaining beagles were euthanized in the same way at 12 weeks after surgery. In total, 24 rear femurs were retrieved. The femoral condylar-implant specimens were used for histological analysis and scanning electron microscopy (SEM) analysis, while the mechanical push-out tests were conducted using the femoral shaft-implant specimens.

### Histological Assessment

The femoral condylar-implant specimens were immediately fixed in 10% formaldehyde for 7 days. After a consecutive series of ethanol dehydration, the specimens were embedded in polymethylacrylate, and then cut into ~100 μm thick sections by using a microtome with a diamond blade (Leica Biosystems, Wetzlar, Germany). Finally, these sections were ground and polished to the ~20 μm thickness for methylene blue and basic fuchsin staining. The formation of new bone at the interface was observed by a light microscope (Olympus BH-2, Olympus America Inc., USA). To quantify the bone formation at the bone–implant interface, the bone–implant contact ratio (BICR) was calculated as the proportion of the bone contact length to the total perimeter of the specimen using an analytical method similar to that described in previous studies.[31,32]

### Push-Out Test

To evaluate the strength of interfacial osseointegration, the mechanical push-out test was carried out. The retrieved bone specimens containing the implants were cut into semi-circular bone–implant blocks, and then placed in a mechanical testing machine (AGS-X, Shimadzu, Japan). Subsequently, 1 KN of axial compressive load was applied to push the implants through the bone at a rate of 1.0 mm/min (cross-head speed) until the bone–implant interface was destroyed. During the period of application of the axial compressive load, the bone–implant interfacial strength was the only force acting against the implant movement. The stress–strain curves were recorded, and the shear modulus of the bone–implant interface was subsequently calculated from the slope of the shear stress versus shear strain plot.

## Statistical Analysis

All the above-mentioned experiments were performed strictly in accordance with the relevant protocols and specifications. All data were analyzed statistically using ANOVA and expressed as the average ± standard deviation with a level of significance of $p < 0.05$.

# Results

## Surface Characteristics

The typical surface morphologies for each sample category are shown in Figure 1C. The EDHA-Ti surface was completely covered with nanoplate-like sediments. However, well-flattened particles along with some spherical particles were deposited on the PSHA-Ti surface. The surface of AA-Ti was characterized by an irregular appearance of a large number of microporous networks. The XRD pattern for each sample category is presented in Figure 2. For the EDHA-Ti samples, the characteristic XRD peaks were relatively similar, the standard pattern for the HA phase (JCPDS No. 09–0432) being exhibited. However, the strongest intensity was located at the (002) surface in the EDHA group. Meanwhile, peaks corresponding to the (002), (210), (211), and (222) planes of HA (JCPDS No. 09–0432) were observed for the PSHA-Ti samples with the (002)/(211) ratio being 0.516. In addition, the XRD pattern for AA-Ti was not in accordance with the

standard pattern for pure Ti (JCPDS No. 44–1294), but had some similarity with the characteristic intensities for anatase (JCPDS No. 21–1272) and rutile (JCPDS No. 21–1276), indicating the phase composition of the AA-treated Ti surface was a mixture of Ti, anatase, and rutile. Relatively higher crystallinity of HA was obtained in the PS-produced coating relative to the ED coating (80.2% vs 48.5%, respectively). Compared to PSHA-Ti, EDHA-Ti had a lower Ca/P ratio. As illustrated in Figure 3A, the surface roughness (Rq) values for EDHA-Ti, PSHA-Ti, and AA-Ti were 798.07 ± 112.52 nm, 104.48 ± 30.20 nm, and 96.62 ± 15.61 nm, respectively (Figure 3). Additionally, the wettability characterization results revealed that the contact angle of EDHA-Ti was approximately 8.5° ± 2.1°, whereas a relatively large contact angle was observed for AA-Ti (21.1° ± 1.1°). However, a near 0° contact angle was observed for PSHA-Ti.

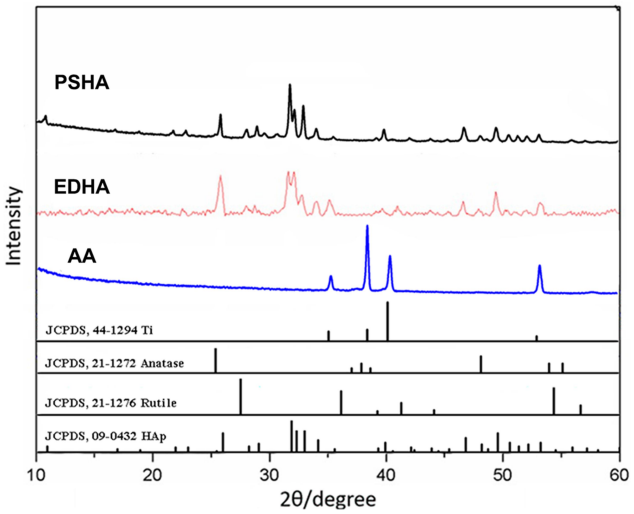


**Figure 2** XRD patterns of titanium samples with different surface modifications.

## Cell Growth and Proliferation of MC3T3-E1

The cell growth curves for MC3T3-E1 cultured in EDHA-Ti, PSHA-Ti, and AA-Ti are presented in Figure 4A. Typical spindle-shaped osteoblasts were visualized for all sample images. On day 3, significantly large number of cells were found for all the sample categories, but it seemed that slightly more cells resided on the PSHA-Ti compared to EDHA-Ti and AA-Ti. After 5 days of consecutive cell culture, all of the samples were almost covered by MC3T3-E1 cells, whereas very few dead cells were observed on these substrates.

According to the results of the CCK-8 assay (Figure 4B), continuous proliferation of MC3T3-E1 osteoblastic cells was observed on the modified surfaces throughout the entire culture period. On the first day, the cells cultured on PSHA-Ti showed the highest rate of cell proliferation. Meanwhile, the proliferative rate of cells cultured with EDHA-Ti was slightly lower compared to AA-Ti. After 3 days of culture, the proliferation of MC3T3-E1 was significantly promoted in each of the sample categories, and proliferation was still slightly greater in PSHA-Ti than in the others. Similar trends in cell proliferation continued to day 5.

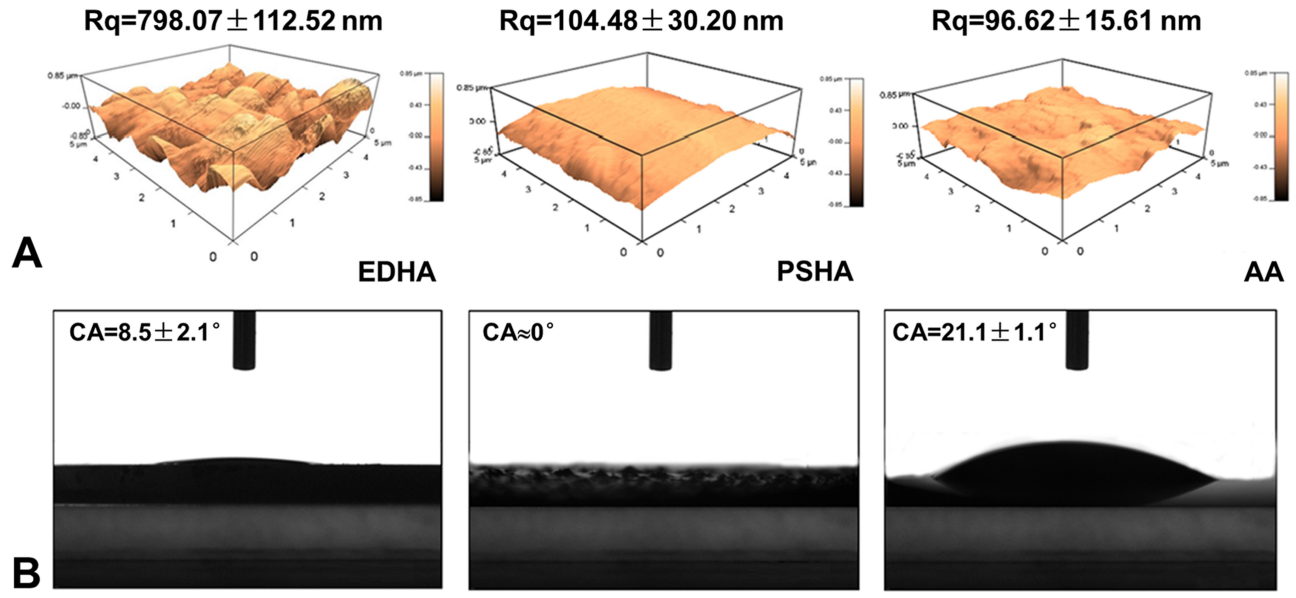


**Figure 3** (**A**) AFM analysis (surface roughness, Rq) and (**B**) contact angle (CA) tests of titanium samples with different surface modifications.

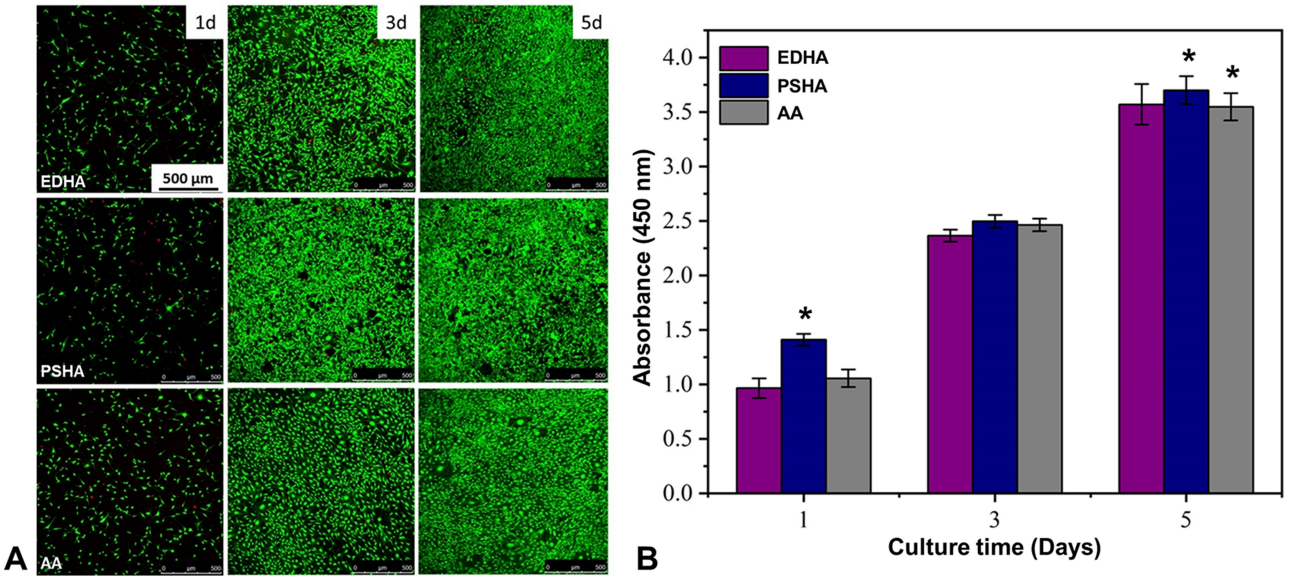


**Figure 4** CLSM images (**A**) and CCK8 analysis for the proliferation (**B**) of MC3T3-E1 cells cultured on titanium samples with different surface modifications (*p < 0.05).

## Osteogenic Differentiation of MC3T3-E1 Cells

The differences in the osteogenic gene expression of MC3T3-E1 cells co-cultured with surface-modified substrates are revealed in Figure 5. Compared to PSHA-Ti, EDHA-Ti with a nanostructured coating significantly enhanced the expression of all osteogenic markers to varying degrees throughout the entire culture period, except for the initial period for OCN expression. EDHA-Ti and AA-Ti had a similar ability to upregulate BSP, Col-I, and OPN expression, whereas the highest expression for ALP and OCN was observed for MC3T3-E1 cells cultured on AA-Ti. Specifically, on day 7, the expression of BSP was higher for MC3T3-E1 cells cultured on EDHA-Ti than on AA-Ti. With extended culture, a higher expression of Col-I was observed for MC3T3-E1 cells cultured on EDHA-Ti compared with that observed for the cells cultured on AA-Ti. Meanwhile, EDHA-Ti showed a lower expression of ALP, BSP, OCN, and OPN compared to AA-Ti. During the whole culture period, PSHA-Ti showed modest effects on the osteogenic differentiation of MC3T3-E1 cells.

## Histology Analysis

Typical light microscopy images of the stained histology sections at 6 and 12 weeks after implantation are presented in Figure 6A. No inflammatory reactions were observed in any of the samples. At 6 weeks after implantation, the amount of new bone formed around the EDHA-Ti implants seemed to be larger than that formed around the PSHA-Ti and the AA-Ti implants. Correspondingly, similar trends were observed in the comparisons for the bone–implant contact ratio (BICR). Specifically, the BICR of EDHA-Ti was slightly higher than the others, and the lowest BICR was observed in the AA-Ti group (Figure 6B). In the case of the extended implantation time, the increase in new bone formation around the samples was observed in all categories, except for the AA-Ti group. Compared with week 6, the greatest increments in the BICR were observed in the implantation of the PSHA-Ti samples, and the final BICR of PSHA-Ti was significantly higher than those of EDHA-Ti and AA-Ti. For EDHA-Ti, there was a small increase in the BICR, but the total BICR was still higher relative that for AA-Ti.

## Mechanical Testing

The push-out tests were performed to investigate the bonding strength of the bone–implant interface, and to calculate the interfacial shear modulus. The results are presented in Figure 7. At week 6, the shear modulus for the PSHA-Ti (21.99 ± 1.77 MPa) was almost 10 times that for the AA-Ti implant (2.22 ± 1.26 MPa). Moreover, a relatively high bonding strength (18.02 ± 4.62 MPa) was observed at same period in the case of the EDHA-Ti implant. However, there was no statistical difference in interfacial shear modulus between the PSHA-Ti and the EDHA-Ti groups. With increase in the implantation period, a further increase in bonding strength was observed in all groups. After 12 weeks of implantation, the highest interfacial shear modulus was still obtained for the PSHA-Ti implantation, which had increased by more than 60%

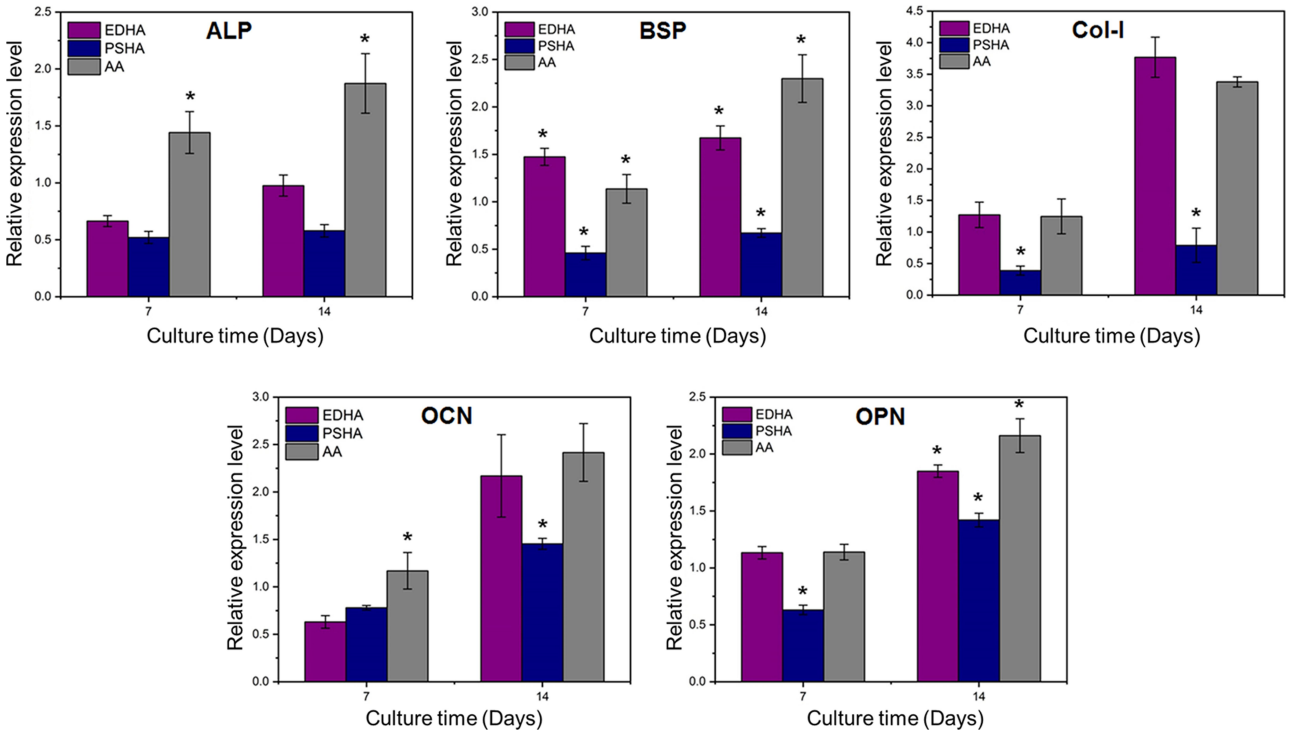


**Figure 5** PCR analysis for the osteogenic gene expressions of MC3T3-E1 cells cultured on titanium samples with different surface modifications (*p < 0.05).

(34.20 ± 2.18 MPa) compared with week 6. In addition, the bonding strength for the EDHA-Ti implant was 24.60 ± 5.30 MPa, an improvement of 33%. Meanwhile, an increase in the bonding strength was observed for the AA-Ti implant at week 12, but the interfacial stability generated by AA-Ti was still the lowest (8.50 ± 2.71 MPa).

## Discussion

Since the reporting of the enhanced osseointegration properties of porous materials in 1972,[33] substantial research has been undertaken on the development of porous Ti for bone repair and regeneration.[9,10,12,34–37] Even though porous Ti minimizes stress shielding and promotes bone ingrowth,[19] the bio-inert nature of Ti and the inferior osseointegration capability still increase the risk of implant failure and affect the lifespan of implants in clinical applications.[38] The appropriate surface modifications need to provide an effective and satisfactory outcome regarding the preparation of bioactive Ti with enhanced osteogenesis and osseointegration capabilities.[34,39] Both acidic and/or alkaline treatments and bioactive HA coatings have been recognized as commendable approaches

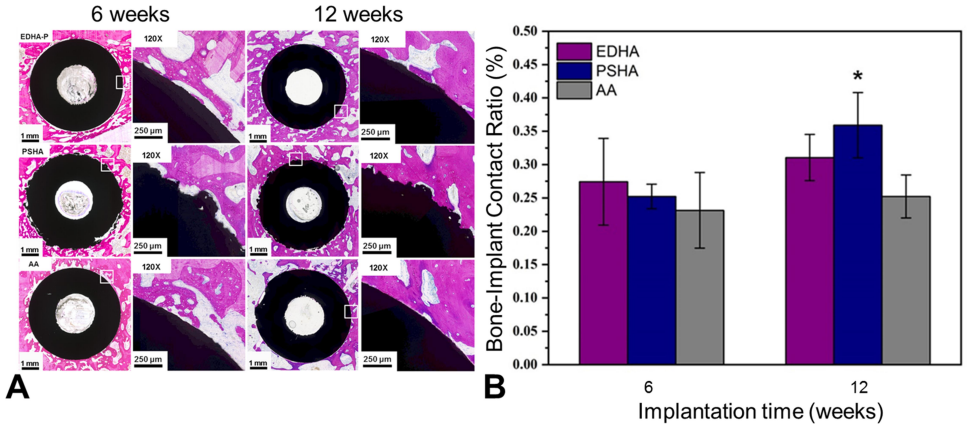


**Figure 6** (**A**) Light microscope images of methylene blue and basic fuchsin stained histological sections of various titanium samples at 6 and 12 weeks postoperatively. (**B**) Quantitative analysis for new bone at the interface area of various titanium samples after in vivo implantation for 6 and 12 weeks (*p < 0.05).

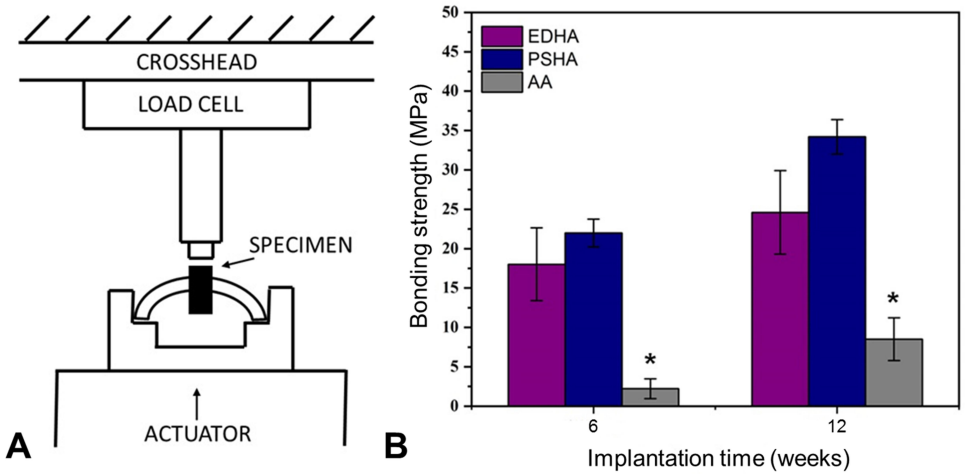


**Figure 7** (**A**) Schematic diagram of push-out tests for the retrieved specimens. (**B**) Bone-implant bonding forces of various titanium samples after in vivo implantation for 6 and 12 weeks (*$p < 0.05$).

for improving the bioactivity of Ti implants.[12,37,40,41] In spite of the risk of delamination, HA coatings are superior to chemical treatments in terms of augmenting osteogenic activity because of the direct release of calcium and phosphate ions. Although various methods have been reported for preparation of HA coatings, the non-line-of-sight coating processes, such as ED, biomimetic, and sol-gel deposition, probably represent the preferred route for current and future clinical use due to the highly increased demand for porous Ti implants. In addition, nanoscale surface modifications have been demonstrated to enhance cell adhesion and tissue ingrowth.[24–26] However, the influence of HA coatings with or without a unified nanotopography on osteogenesis and osseointegration at the bone–implant interface is not clear yet. In this study, nanoplate-like HA coatings were prepared on Ti with a $TiO_2$ layer by a combination of an ED method and an AA pretreatment. Thereafter, the osteogenic activity and the interfacial osteointegration properties of the nanoplate-like EDHA coatings were systematically investigated by undertaking comparison studies with nanotopography-free PSHA coatings and AA treatments through in vitro and vivo experiments.

The surface topography and chemical composition of the surface-modified structures are crucial to achieving bioactivity of the implants.[42,43] The surface of PSHA-Ti exhibited a lamellar structure with irregularly distributed spherical particles (Figure 1C), which became well-flattened due to their high-speed on striking the substrate after undergoing melting in the plasma jet. No nanotopographical features were observed in the products of the PS method. Conversely, uniform nanoplate-like HA sediments were successfully prepared by the ED method with a pulse current density of 5 mA/cm$^2$ (Figure 1C). Although the critical roles of a low current density in fabricating a HA coating with a plate-like structure have been revealed,[44,45] most of the plate-like HA production was at the microscale rather than at the nanoscale level. Recently, the fabrication techniques and preliminary biological evaluation of nanostructured HA coatings have been discussed. Wang and Eliaz successfully modified a Ti surface with a nanostructured HA coating using a standard three-electrode cell containing 0.61 mM $Ca(NO_3)_2$ and 0.36 mM $NH_4H_2PO_4$ at 85°C.[45] Although a direct comparison between the plate-like nanostructured HA coating prepared in the study of Wang and Eliaz and that of the present study was not possible due to the lack of details concerning the deposition conditions of the former, the relatively high similarities of the respective nanostructures as evidenced by the respective SEM images (Figure 1C), give preliminarily confirmation of the suitability of the present approach. Furthermore, the amount of sediment per unit area in this study may be larger than that of Wang and Eliaz, and this may be more beneficial in terms of increasing the surface roughness and consequently promoting cell adhesion.

The results for XRD analysis (Figure 2) confirmed that the phase composition of the sediments on EDHA-Ti and PSHA-Ti was HA. However, the growth direction of the HA crystals was apparently different between these two types of HA coatings. EDHA-Ti had the highest intensity at the (002) surface, indicating that the HA crystal was

grown with (002) being the preferred orientation, and thus was perpendicular to the surface. In contrast, for PSHA-Ti, the strongest intensity was located at the (211) plane, and the (002)/(211) ratio was less than 0.52 in the XRD pattern. Thus, the orientation of the HA crystal growth was nearly horizontal to the surface, which corresponds to the lamellar morphology of the standard PS-produced HA coatings. However, previous studies revealed that HA crystals with a (002) preferred orientation showed superior mechanical properties, including a higher hardness, a higher elastic modulus, and a higher fracture toughness, compared with normal HA coatings.[46–48] Besides the mechanical advantages, the enhancement of cell adhesion and attachment could be further strengthened by the (002)-orientated HA coatings.[49]

Generally, surface wettability has been correlated with the adhesion and proliferation of osteoblasts, and cells exhibit a strong preference for hydrophilic surfaces.[50] PSHA-Ti displayed super-hydrophilicity properties (Figure 3). Moreover, a reduction of the water-contact angle in the nanostructured EDHA coating compared to AA-Ti (Figure 3) was confirmed. Besides, given the conferred benefits of the nanoscale surface on hydrophilicity,[51,52] the plate-like nanostructures vertical to the substrate may play a critical role in further improving the hydrophilicity of the samples in this study. Thus, both EDHA and PSHA coatings had a high potential to facilitate cell adhesion and proliferation.

The CLSM observation and CCK-8 experiments confirmed that the growth and proliferation of MC3T3-E1 osteoblastic cells cultured on EDHA-Ti became as satisfactory as that for cells on PSHA-Ti with an increase in the culture period (Figure 4). Although the proliferative rate for cells on EDHA-Ti was lower than that of PSHA-Ti on day 1, a similar proliferation level was observed in EDHA-Ti and PSHA-Ti for an extended culture period. During the entire culture period, a comparable proliferation capability was observed between AA-Ti and EDHA-Ti. The positive effect of a nanostructured surface on cell adhesion is well known. Compared to a flat surface of Ti, a nanotube-like surface promoted more cell adhesion. This increase in cell adhesion might be related to the increased surface-to-volume ratio and the wettability caused by the tube-like topography.[53,54] Moreover, nanophase biomaterials with diameters less than 100 nm were reported to enhance cell adhesion by increasing the surface energy.[55]

The proliferative response could be affected by some morphological characteristics, such as dimensions, spacings between the adjacent nanostructures, and surface roughness.[53,56] Among these factors, surface roughness was a major factor in affecting the cell proliferation activity. However, the effect of surface roughness at the nanoscale on the cell proliferative rate is still controversial. A negative effect of nanoscale roughness on the cell proliferative rate was reported by Washburn.[56] Moreover, Rq values of 0.5–13 nm dramatically reduced osteoblast cell proliferation. These findings were consistent with our results. Although EDHA-Ti presented the roughest surface (Rq, 798.07 ± 112.52 nm), the proliferative response of EDHA-Ti was weaker than that of PSHA-Ti (Rq, 104.48 ± 30.20 nm). Whist, some studies reported no correlation of cell proliferation rate with nanoscale roughness, and a surface with a mixture of micro/nanoscale surface roughness might promote proliferation.[42,57,58] Therefore, EDHA-Ti with a basic AA-treated surface, which was characterized as having a mixture of micro/nanoscale roughness, will continue to promote cell adhesion and proliferation even if delamination of the coating occurs.

Compared to a previous report on a $TiO_2$ surface with nanotube-like or hemispherical nanostructures,[59–63] it is believed that EDHA-Ti with plate-like nanostructures exhibits a relatively greater propensity to promote cell adhesion and proliferation due to the following reasons: (1) The contact angle for EDHA-Ti observed in our study is apparently smaller than that for Ti nanotubes observed in previous studies (8.5° versus 10.76–24.62°),[61] and cells show a strong preference for attachment and proliferation on a relatively higher hydrophilic surface. (2) The surface-to-volume ratio is significantly higher for a plate shape than for a tube shape, and a higher surface-to-volume ratio is beneficial for providing a relatively more effective surface area for cell attachment and proliferation. (3) The interspacing distances which allow cell proliferation may be larger for plate-like morphology than those for tube-like, rod-like, and hemispherical morphologies. (4) A further reason is that the bioactive material (HA) deposited on the EDHA-Ti surface could more directly and effectively increase the adhesion and proliferative response of osteoblast cells because of the release of calcium and phosphate ions.

Enhanced osteogenic differentiation on EDHA-Ti and AA-Ti was observed in this study. Osteogenic activity for both EDHA-Ti and AA-Ti was significantly higher than that for PSHA-Ti. Furthermore, strong positive effects were observed for the nanoplate-like surface on the early or intermediate period of osteogenic differentiation via the

RT-PCR analysis of ALP, BSP, and Col-I (Figure 5). Although these markers play slightly different roles in bone mineralization or formation,[64,65] the early or intermediate stage is the common acting time-point. Thus, enhanced early-stage osteogenic activity of EDHA-Ti was confirmed. However, a similar up-regulation of osteoblast-specific gene expression caused by nanoscale topography was reported previously. The hemispherical nanostructures of $TiO_2$ enhanced the RUNX2, Osterix, OPN, and BSP expression.[66,67] Besides, the ALP expression and production were significantly increased by the nanotube-like morphology of Ti.[67] Although the consistent trends of osteoblast-specific gene expression up-regulated by the nanostructured surface were confirmed in the present study and previous study, it is believed that the nanostructured HA coating prepared in this work should present better performance on induction of osteogenesis compared to $TiO_2$ with nanotopography and an HA coating without nanotopography.

The strong promotion of early bone formation and also good osseointegration in the EDHA-Ti samples was validated by the histology. According to the histological analysis (Figure 6B), the new bone was formed greatly in the first six weeks for all groups. At this time, the BICR for EDHA-Ti was even higher than that for PSHA-Ti, which may be related to the early promotion of osteogenic expression and differentiation induced by the nanoplate-like surface of EDHA-Ti. However, the amount of new bone formation around PSHA-Ti was slightly more than that around EDHA-Ti after 12 weeks of implantation. No obvious increase in bone growth was observed for the AA-Ti samples even for the increased implantation time of 12 weeks. It was clearly verified that the HA coating could greatly promote new bone formation. Enhanced early-stage osseointegration in the EDHA-Ti was also observed. However, the correlation between the topographical properties of the Ti nanostructures and the promotion of bone contact has been investigated in previous studies. Lin et al compared the interfacial bone contact between nanotubular, nanosponge-like, nanonest-like, and normal Ti, and better osseointegration ability was observed for the nanonest-like and nanotube structured surfaces.[68] Similar results were also reported by other researchers.[69,70] Recently, Bose et al suggested that osseointegration could be further enhanced by introducing a calcium phosphate coating on the $TiO_2$ nanotubes.[71] Thus, it is believed that the nanostructured HA coating on $TiO_2$ prepared in this study may be relatively more effective for inducing bone integration compared with a normal HA coating and a $TiO_2$ surface with nanotopography.

Based on the BICR analysis, higher interfacial strength was observed for the PSHA-Ti samples compared to the EDHA-Ti samples (Figure 7B). However, the bonding strengths (18.02 ± 4.62 MPa at week 6, 24.60 ± 5.30 MPa at week 12) calculated for the EDHA-Ti group were nearly nine- to ten-fold higher compared to those calculated for AA-Ti. Similarly, the push-out test performed in the study of Bjursten et al, indicating that the bonding strength of the $TiO_2$ nanotubes was nine times more than that of a grit-blasted surface.[70] Furthermore, Parcharoen et al successfully fabricated nanoplate-like HA coatings based on nanotube-like $TiO_2$ by ED, and the highest bonding strength recorded was under 20 MPa.[72] Compared to the study conducted by Parcharoen, EDHA-Ti prepared in the present study had a relatively higher interfacial stability after 12 weeks of implantation. However, the present study revealed a mismatch between the results of osteogenic differentiation, BICR, and bonding strength for AA-Ti. The in vitro cellular experiments demonstrated the excellent osteogenic promotion ability of AA-Ti, but the osseointegration after the in vivo implantation of AA-Ti was not acceptable. The interfacial strength observed for the AA-Ti group was significantly lower than the interfacial strengths observed for the other two groups. This indicated the important role of the HA coating in enhancing the osseointegration of the Ti implants. On the one hand, compared with the AA treatment, both the other HA coatings caused an increase in the surface roughness of the substrate and thus promoted the mechanical interlock between the bone and the implant. On the other hand, compared with the AA-Ti, both the EDHA-Ti and the PSHA-Ti caused an increase in new bone growth around the implant and thus promoted biological fixation. Therefore, the HA coating exhibited better osseointegration than the AA treatment. However, because the AA treatment up-regulated the osteogenic activity of MC3T3-E1 cells, the osseointegration ability of AA-Ti might be improved with an increase in the implantation period. Previously, Zhao et al reported that porous Ti with AA treatment exhibited good osteoinduction after implantation into the dorsal muscles of adult dogs for three months.[12]

The degradation rate of the nanostructured HA coating on porous or dense Ti substrates should be further investigated, given that this might provide an explanation for the undesirable change in the BICR after six weeks of implantation in the case of the EDHA-Ti samples.

Clearly, the line-of-sight PS process did not access the interior coating of the porous structure. Therefore, a dense Ti-substrate was used as a basic and common material for preparing the HA coating to directly compare the biological response of EDHA-Ti with those of PSHA-Ti and AA-Ti. However, the procedures and production quality of the EDHA coatings on the porous Ti-samples were relatively similar to those of the ED-fabricated HA coatings on the dense Ti-substrate. Thus, the ED used in this study was also available for the HA coating of porous implants.

## Conclusions

The plate-like nanostructures of the HA coating could significantly enhance the early stage osteogenic differentiation of MC3T3-E1 cells and the osseointegration properties of the bone–implant interface, both of which were demonstrated to be greatly beneficial to improving the initial biomechanical stability of the implants. Considering the superior osteogenic performance and advantageous of a non-line-of-sight process, the nanostructured HA coatings produced by ED could be an alternative choice of surface modification for the clinical use of porous metallic implants, which would probably result in a prolonging of the life-span of these implants.

## Abbreviations

HA, hydroxyapatite; ED, electrodeposition; PS, plasma spraying; Ti, titanium; SEM, scanning electron microscopy; XRD, X-ray diffraction; AFM, atomic force microscope; CLSM, confocal laser scanning microscope; ALP, alkaline phosphatase; OCN, osteocalcin; OPN, osteopontin; BSP, bone sialoprotein; Col-I, collagen I; RT-PCR, real-time quantitative PCR; GAPDH, glyceraldehyde 3-phosphate dehydrogenase; BICR, bone–implant contact ratio.

## Author Contributions

All authors made substantial contributions to conception and design, acquisition of data, or analysis and interpretation of data; took part in drafting the article or revising it critically for important intellectual content; agreed to submit to the current journal; gave final approval of the version to be published; and agree to be accountable for all aspects of the work.

## Funding

This work was financially supported by the National Natural Science Foundation of China (81671825) and the Sichuan Science and Technology Innovation Team of China (2019JDTD0008).

## Disclosure

The authors report no conflicts of interest in this work.

## References

1. Brown SA, Lemons JE. Medical applications of titanium and its alloys: the material and biological issues. West Conshohocken, PA: ASTM; 1996.
2. Okazaki Y, Ito Y, Kyo K, Tateishi T. Corrosion resistance and corrosion fatigue strength of new titanium alloys for medical implants without V and Al. *Mater Sci Eng A*. 1996;213(1–2):138–147. doi:10.1016/0921-5093(96)10247-1
3. Wang X-H, Li J-S, Hu R, Kou H-C, Zhou L. Mechanical properties of porous titanium with different distributions of pore size. *Trans Nonferrous Met Soc China*. 2013;23(8):2317–2322. doi:10.1016/S1003-6326(13)62735-1
4. Rubstein AP, Makarova EB, Trakhtenberg IS, et al. Osseointegration of porous titanium modified by diamond-like carbon and carbon nitride. *Diam Relat Mater*. 2012;22:128–135. doi:10.1016/j.diamond.2011.12.030
5. Camargo WA, Takemoto S, Hoekstra JW, et al. Effect of surface alkali-based treatment of titanium implants on ability to promote in vitro mineralization and in vivo bone formation. *Acta Biomater*. 2017;57:511–523. doi:10.1016/j.actbio.2017.05.016
6. Albayrak O, El-Atwani O, Altintas S. Hydroxyapatite coating on titanium substrate by electrophoretic deposition method: effects of titanium dioxide inner layer on adhesion strength and hydroxyapatite decomposition. *Surf Coat Technol*. 2008;202(11):2482–2487. doi:10.1016/j.surfcoat.2007.09.031
7. Oh I-H, Nomura N, Chiba A, et al. Microstructures and bond strengths of plasma-sprayed hydroxyapatite coatings on porous titanium substrates. *J Mater Sci Mater Med*. 2005;16(7):635–640. doi:10.1007/s10856-005-2534-4
8. Zhao CY, Zhu XD, Yuan T, Fan HS, Zhang XD. Fabrication of biomimetic apatite coating on porous titanium and their osteointegration in femurs of dogs. *Mater Sci Eng C*. 2010;30(1):98–104. doi:10.1016/j.msec.2009.09.004
9. Fujibayashi S, Neo M, Kim H-M, Kokubo T, Nakamura T. Osteoinduction of porous bioactive titanium metal. *Biomaterials*. 2004;25(3):443–450. doi:10.1016/S0142-9612(03)00551-9
10. Takemoto M, Fujibayashi S, Neo M, et al. Osteoinductive porous titanium implants: effect of sodium removal by dilute HCl treatment. *Biomaterials*. 2006;27(13):2682–2691. doi:10.1016/j.biomaterials.2005.12.014
11. Wu J-M, Hayakawa S, Tsuru K, Osaka A. Low-temperature preparation of anatase and rutile layers on titanium substrates and their ability to induce in vitro apatite deposition. *J Am Ceram Soc*. 2004;87(9):1635–1642. doi:10.1111/j.1551-2916.2004.01635.x
12. Zhao C, Zhu X, Liang K, et al. Osteoinduction of porous titanium: a comparative study between acid-alkali and chemical-thermal treatments. *J Biomed Mater Res B Appl Biomater*. 2010;95(2):387–396. doi:10.1002/jbm.b.31728
13. Kim HM, Kokubo T, Fujibayashi S, Nishiguchi S, Nakamura T. Bioactive macroporous titanium surface layer on titanium substrate. *J Biomed Mater Res*. 2000;52(3):553–557. doi:10.1002/1097-4636(20001205)52:3<553::AID-JBM14>3.0.CO;2-X
14. Uchida M, Kim H-M, Kokubo T, Fujibayashi S, Nakamura T. Effect of water treatment on the apatite-forming ability of NaOH-treated titanium metal. *J Biomed Mater Res*. 2002;63(5):522–530. doi:10.1002/jbm.10304

15. Lu Y-P, Li M-S, Li S-T, Wang Z-G, Zhu R-F. Plasma-sprayed hydroxyapatite+ titania composite bond coat for hydroxyapatite coating on titanium substrate. *Biomaterials*. 2004;25(18):4393–4403. doi:10.1016/j.biomaterials.2003.10.092
16. Kokubo T, Yamaguchi S. Bioactive metals prepared by surface modification: preparation and properties. In: *Applications of Electrochemistry and Nanotechnology in Biology and Medicine I*. Springer; 2011:377–421.
17. Barre`Re F, Layrolle P, Blitterswijk CAV, Groot KD. Biomimetic coatings on titanium: a crystal growth study of octacalcium phosphate. *J Mater Sci Mater Med*. 2001;12(6):529–534. doi:10.1023/a:1011271713758
18. Eliaz N, Sridhar T, Kamachi Mudali U, Raj B. Electrochemical and electrophoretic deposition of hydroxyapatite for orthopaedic applications. *Surf Eng*. 2005;21(3):238–242. doi:10.1179/174329405X50091
19. Domínguez-Trujillo C, Peón E, Chicardi E, et al. Sol-gel deposition of hydroxyapatite coatings on porous titanium for biomedical applications. *Surf Coat Technol*. 2018;333:158–162. doi:10.1016/j.surfcoat.2017.10.079
20. Sun L, Berndt CC, Gross KA, Kucuk A. Material fundamentals and clinical performance of plasma-sprayed hydroxyapatite coatings: a review. *J Biomed Mater Res*. 2001;58(5):570–592. doi:10.1002/jbm.1056
21. Palka V, Poštrková E, Koerten H. Some characteristics of hydroxylapatite powder particles after plasma spraying. *Biomaterials*. 1998;19(19):1763–1772. doi:10.1016/S0142-9612(98)00087-8
22. Ellies L, Nelson D, Featherstone J. Crystallographic changes in calcium phosphates during plasma-spraying. *Biomaterials*. 1992;13(5):313–316. doi:10.1016/0142-9612(92)90055-S
23. Mali S, Nune K, Misra R. Biomimetic nanostructured hydroxyapatite coatings on metallic implant materials. *Mater Technol*. 2016;31(13):782–790. doi:10.1080/10667857.2016.1224609
24. Tran N, Webster TJ. Nanotechnology for bone materials. *Wiley Interdiscip Rev Nanomed Nanobiotechnol*. 2009;1(3):336–351. doi:10.1002/wnan.23
25. Wang N, Li H, Lü W, et al. Effects of TiO2 nanotubes with different diameters on gene expression and osseointegration of implants in minipigs. *Biomaterials*. 2011;32(29):6900–6911. doi:10.1016/j.biomaterials.2011.06.023
26. Park J, Bauer S, von der Mark K, Schmuki P. Nanosize and vitality: TiO2 nanotube diameter directs cell fate. *Nano Lett*. 2007;7(6):1686–1691. doi:10.1021/nl070678d
27. Adam M, Ganz C, Xu W, Sarajian H-R, Götz W, Gerber T. In vivo and in vitro investigations of a nanostructured coating material–a preclinical study. *Int J Nanomedicine*. 2014;9:975. doi:10.2147/IJN.S48416
28. Raines AL, Olivares-Navarrete R, Wieland M, Cochran DL, Schwartz Z, Boyan BD. Regulation of angiogenesis during osseointegration by titanium surface microstructure and energy. *Biomaterials*. 2010;31(18):4909–4917. doi:10.1016/j.biomaterials.2010.02.071
29. Tan A, Pingguan-Murphy B, Ahmad R, Akbar S. Review of titania nanotubes: fabrication and cellular response. *Ceram Int*. 2012;38(6):4421–4435. doi:10.1016/j.ceramint.2012.03.002
30. Chen H, Wang C, Yang X, et al. Construction of surface HA/TiO2 coating on porous titanium scaffolds and its preliminary biological evaluation. *Mater Sci Eng C Mater Biol Appl*. 2017;70(Pt 2):1047–1056. doi:10.1016/j.msec.2016.04.013
31. Yuan B, Cheng Q, Zhao R, et al. Comparison of osteointegration property between PEKK and PEEK: effects of surface structure and chemistry. *Biomaterials*. 2018;170:116–126. doi:10.1016/j.biomaterials.2018.04.014
32. Raffa ML, Nguyen V-H HG. Micromechanical modeling of the contact stiffness of an osseointegrated bone–implant interface. *Biomed Eng Online*. 2019;18(1):114. doi:10.1186/s12938-019-0733-3
33. Weber JN, White EW. Carbon-metal graded composites for permanent osseous attachment of non-porous metals. *Mater Res Bull*. 1972;7(9):1005–1016. doi:10.1016/0025-5408(72)90092-X
34. Karaji ZG, Houshmand B, Faghihi S. Surface modification of porous titanium granules for improving bioactivity. *Int J Oral Maxillofac Implants*. 2016;31(6):1274–1280. doi:10.11607/jomi.5246
35. Kawai T, Takemoto M, Fujibayashi S, et al. Osteoinduction on acid and heat treated porous Ti metal samples in canine muscle. *PLoS One*. 2014;9(2):e88366. doi:10.1371/journal.pone.0088366
36. Tamaddon M, Samizadeh S, Wang L, Blunn G, Liu C. Intrinsic osteoinductivity of porous titanium scaffold for bone tissue engineering. *Int J Biomater*. 2017;2017:5093063. doi:10.1155/2017/5093063
37. Yao Y-T, Liu S, Swain MV, Zhang XP, Zhao K, Jian YT. Effects of acid-alkali treatment on bioactivity and osteoinduction of porous titanium: an in vitro stud. *Mater Sci Eng C*. 2019;94:200–210. doi:10.1016/j.msec.2018.08.056
38. Saini M, Singh Y, Arora P, Arora V, Jain K. Implant biomaterials: a comprehensive review. *World J Clin Cases*. 2015;3(1):52–57. doi:10.12998/wjcc.v3.i1.52
39. Liu X, Chu PK, Ding C. Surface modification of titanium, titanium alloys, and related materials for biomedical applications. *Mater Sci Eng R Rep*. 2004;47(3–4):49–121. doi:10.1016/j.mser.2004.11.001
40. Kattimani VS, Kondaka S, Lingamaneni KP. Hydroxyapatite–Past, present, and future in bone regeneration. *Bone Tissue Regener Insights*. 2016;7(BTRI):S36138. doi:10.4137/BTRI.S36138
41. Ripamonti U, Roden LC, Renton LF. Osteoinductive hydroxyapatite-coated titanium implants. *Biomaterials*. 2012;33(15):3813–3823. doi:10.1016/j.biomaterials.2012.01.050
42. Biggs M, Richards R, Gadegaard N, et al. Interaction with nanoscale topography: adhesion quantification and signal transduction in cells of osteogenic and multipotent lineage. *J Biomed Mater Res A*. 2009;91:195–208. doi:10.1002/jbm.a.32196
43. Xu JY, Chen XS, Zhang CY, Liu Y, Wang J, Deng FL. Improved bioactivity of selective laser melting titanium: surface modification with micro-/nano-textured hierarchical topography and bone regeneration performance evaluation. *Mater Sci Eng C*. 2016;68:229–240. doi:10.1016/j.msec.2016.05.096
44. Kuo M, Yen S. The process of electrochemical deposited hydroxyapatite coatings on biomedical titanium at room temperature. *Mater Sci Eng C*. 2002;20(1–2):153–160. doi:10.1016/S0928-4931(02)00026-7
45. Wang H, Eliaz N, Hobbs LW. The nanostructure of an electrochemically deposited hydroxyapatite coating. *Mater Lett*. 2011;65(15–16):2455–2457. doi:10.1016/j.matlet.2011.05.016
46. Wang Y, Liu X, Fan T, Tan Z, Zhou Z, He D. In vitro evaluation of hydroxyapatite coatings with (002) crystallographic texture deposited by micro-plasma spraying. *Mater Sci Eng C*. 2017;75:596–601. doi:10.1016/j.msec.2017.02.119
47. Kim H, Camata RP, Chowdhury S, Vohra YK. In vitro dissolution and mechanical behavior of c-axis preferentially oriented hydroxyapatite thin films fabricated by pulsed laser deposition. *Acta Biomater*. 2010;6(8):3234–3241. doi:10.1016/j.actbio.2010.02.031
48. Liu X, He D, Zhou Z, et al. Characteristics of (002) oriented hydroxyapatite coatings deposited by atmospheric plasma spraying. *Coatings*. 2018;8(8):258. doi:10.3390/coatings8080258
49. Kim H, Camata RP, Lee S, et al. Calcium phosphate bioceramics with tailored crystallographic texture for controlling cell adhesion. In: *MRS Online Proceedings Library Archive*. 2006:925.
50. Lim JY, Liu X, Vogler EA, Donahue HJ. Systematic variation in osteoblast adhesion and phenotype with substratum surface characteristics. *J Biomed Mater Res A*. 2004;68(3):504–512. doi:10.1002/jbm.a.20087
51. Lin K, Xia L, Gan J, et al. Tailoring the nanostructured surfaces of hydroxyapatite bioceramics to promote protein adsorption, osteoblast growth, and osteogenic differentiation. *ACS Appl Mater Interfaces*. 2013;5(16):8008–8017. doi:10.1021/am402089w

52. Xia L, Lin K, Jiang X, et al. Effect of nano-structured bioceramic surface on osteogenic differentiation of adipose derived stem cells. *Biomaterials*. 2014;35(30):8514–8527. doi:10.1016/j.biomaterials.2014.06.028
53. Brammer KS, Oh S, Cobb CJ, Bjursten LM, van der Heyde H, Jin S. Improved bone-forming functionality on diameter-controlled TiO(2) nanotube surface. *Acta Biomater*. 2009;5(8):3215–3223. doi:10.1016/j.actbio.2009.05.008
54. Yao C, Perla V, McKenzie J, Slamovich E, Webster T. Anodized Ti and Ti6Al4V possessing nanometer surface features enhance osteoblast adhesion. *J Biomed Nanotechnol*. 2005;1:68–73. doi:10.1166/jbn.2005.008
55. Khang D, Lu J, Yao C, Haberstroh KM, Webster TJ. The role of nanometer and sub-micron surface features on vascular and bone cell adhesion on titanium. *Biomaterials*. 2008;29(8):970–983. doi:10.1016/j.biomaterials.2007.11.009
56. Washburn N, Yamada K, Simon C, Kennedy S, Amis E. High-throughput investigation of osteoblast response to polymer crystallinity: influence of nanometer-scale roughness on proliferation. *Biomaterials*. 2004;25:1215–1224. doi:10.1016/j.biomaterials.2003.08.043
57. Zhao G, Zinger O, Schwartz Z, Wieland M, Landolt D, Boyan B. Osteoblast-like cells are sensitive to submicron-scale surface structure. *Clin Oral Implants Res*. 2006;17:258–264. doi:10.1111/j.1600-0501.2005.01195.x
58. Zinger O, Zhao G, Schwartz Z, et al. Differential regulation of osteoblasts by substrate microstructural features. *Biomaterials*. 2005;26(14):1837–1847. doi:10.1016/j.biomaterials.2004.06.035
59. Lewis G. Nanostructured hydroxyapatite coating on bioalloy substrates: current status and future directions. *J Adv Nanomater*. 2017. doi:10.22606/jan.2017.21007
60. Liang Y, Yang X, Cui Z, Zhu S. Effect of TiO2 nanotube morphology on the formation of apatite layer in simulated body fluid. *Curr Nanosci*. 2010;6(3):256–261. doi:10.2174/157341310791171144
61. Shin DH, Shokuhfar T, Choi CK, Lee SH, Friedrich C. Wettability changes of TiO2 nanotube surfaces. *Nanotechnology*. 2011;22:315704. doi:10.1088/0957-4484/22/31/315704
62. Su E, Justin D, Pratt C, et al. Effects of titanium nanotubes on the osseointegration, cell differentiation, mineralisation and antibacterial properties of orthopaedic implant surfaces. *Bone Joint J*. 2018;100-B:9–16. doi:10.1302/0301-620X.100B1.BJJ-2017-0551.R1
63. Wang J, Meng F, Song W, et al. Nanostructured titanium regulates osseointegration via influencing macrophage polarization in the osteogenic environment. *Int J Nanomedicine*. 2018;13:4029–4043. doi:10.2147/IJN.S163956
64. Xia L, Lin K, Jiang X, et al. Enhanced osteogenesis through nano-structured surface design of macroporous hydroxyapatite bioceramic scaffolds via activation of ERK and p38 MAPK signaling pathways. *J Mater Chem B*. 2013;1(40):5403–5416. doi:10.1039/c3tb20945h
65. Scherberich A, Müller AM, Schäfer DJ, Banfi A, Martin I. Adipose tissue-derived progenitors for engineering osteogenic and vasculogenic grafts. *J Cell Physiol*. 2010;225(2):348–353. doi:10.1002/jcp.22313
66. Tambasco de Oliveira P, Nanci A. Nanotexturing of titanium-based surfaces upregulates expression of bone sialoprotein and osteopontin by cultured osteogenic cells. *Biomaterials*. 2004;25(3):403–413. doi:10.1016/S0142-9612(03)00539-8
67. Guo J, Padilla RJ, Ambrose W, De Kok IJ, Cooper LF. The effect of hydrofluoric acid treatment of TiO2 grit blasted titanium implants on adherent osteoblast gene expression in vitro and in vivo. *Biomaterials*. 2007;28(36):5418–5425. doi:10.1016/j.biomaterials.2007.08.032
68. Lin L, Wang H, Ni M, et al. Enhanced osteointegration of medical titanium implant with surface modifications in micro/nanoscale structures. *J Orthop Translat*. 2014;2(1):35–42. doi:10.1016/j.jot.2013.08.001
69. Alves-Rezende M, Capalbo L, Limírio J, Capalbo B, Limírio P, Rosa J. The role of TiO2 nanotube surface on osseointegration of titanium implants: biomechanical and histological study in rats. *Microsc Res Tech*. 2020;83(7):817–823. doi:10.1002/jemt.23473
70. Bjursten LM, Rasmusson L, Oh S, Smith GC, Brammer KS, Jin S. Titanium dioxide nanotubes enhance bone bonding in vivo. *J Biomed Mater Res A*. 2010;92(3):1218–1224. doi:10.1002/jbm.a.32463
71. Bose S, Banerjee D, Shivaram A, Tarafder S, Bandyopadhyay A. Calcium phosphate coated 3D printed porous titanium with nanoscale surface modification for orthopedic and dental applications. *Mater Des*. 2018;151:102–112. doi:10.1016/j.matdes.2018.04.049
72. Parcharoen Y, Termsuksawad P, Sirivisoot S. Improved bonding strength of hydroxyapatite on titanium dioxide nanotube arrays following alkaline pretreatment for orthopedic implants. *J Nanomater*. 2016;2016:9143969. doi:10.1155/2016/9143969